

Dynamically localized systems: entanglement exponential sensitivity and efficient quantum simulations.

Simone Montangero*

NEST-INFM & Scuola Normale Superiore, Piazza dei Cavalieri 7, 56126 Pisa, Italy

(Dated: December 20, 2018)

We study the pairwise entanglement present in a quantum computer that simulates a dynamically localized system. We show that the concurrence is exponentially sensitive to changes in the Hamiltonian of the simulated system. Moreover, concurrence is exponentially sensitive to the “logic” position of the qubits chosen. These sensitivities could be experimentally checked efficiently by means of quantum simulations with less than ten qubits. We also show that the feasibility of efficient quantum simulations is deeply connected to the dynamical regime of the simulated system.

PACS numbers: 05.45.Mt, 03.67.Mn, 03.67.Lx, 07.05.Tp

The study of the entanglement in quantum chaotic systems is object of growing interests [1]. These works are based on classical simulations of quantum systems. Developing quantum computers will enhance our investigations power giving the possibility of performing nowadays unaccessible simulations. However, being able to perform exact quantum computation is not a sufficient condition to assure that quantum simulations will be useful: extracting useful information in an efficient way is a difficult task that, in some cases, drastically decreases the efficiency of quantum algorithms [2, 3]. Moreover, in [4] it has been shown that the entanglement present in a quantum system plays an important role in the possibility of performing efficient classical simulations of quantum systems. Thus, the presence of entanglement and the processes of quantum measurement may determine the efficiency of quantum algorithms.

It is well known that quantum chaotic systems display exponential sensitivity to small changes of the Hamiltonian [5] in dynamical quantities as the fidelity [6]. In [7] it has been shown that the entanglement evolution is influenced by the presence of quantum chaos in a system following the characteristic decays of the fidelity. This result has been found in a system with no classical analogue. Here, we study the concurrence evolution between the qubits in a quantum computer that is running a quantum algorithm to simulate a quantum chaotic system, in the regime where dynamical localization occurs. Dynamical localization is another signature of quantum chaos: it has been first predicted in [10], and experimentally observed in cold atoms [11]. It has been related to Anderson localization [12] of electrons in disordered crystals. Then, it is interesting to perform simulation on many-body or classically chaotic quantum system to check whenever they localize or not: The analysis of localization length as a function of the parameters of the system is important to study transport phenomena. In [3] it has been shown that localization length can be extracted with poly-

mial gain if an efficient quantum algorithm to simulate the system exists. This is not a trivial property, as the efficient extracion of many interesting quantities is precluded due to the exponential number of measurements needed to know all the wave function coefficients.

In this paper we show that the presence of an exponentially localized wave function implies exponentially sensitivity in the concurrence between qubits. This sensitivity is both with respect to small changes in the Hamiltonian and to the pair of qubits chosen. The pairwise entanglement can be extracted efficiently from any quantum algorithm that simulates a quantum system efficiently. Indeed, the measure of the reduced density matrix of two qubits is an efficient process that does not scale with the size of the system. Thus, both localization length and concurrence can be measured efficiently by means of quantum simulations. We also study the entanglement of blocks of qubits with respect of the other and we show that these properties are strictly related to the localization length. Thus, following [4], the localization length determine the feasibility of efficient classical simulation of the system.

The Quantum Sawtooth Map (QSM) is a suitable model of quantum chaotic system that displays dynamical localization which can be efficiently simulated with a quantum computer. The QSM belongs to the kicked map family and it is defined by the Hamiltonian

$$\hat{H}(t) = \frac{\hat{n}^2}{2} + k \frac{(\hat{\theta} - \pi)^2}{2} \sum_r \delta(t - rT), \quad (1)$$

where $\delta_T(t)$ is a delta of Dirac and $r \in \text{Re}$, \hat{n} and $\hat{\theta}$ are canonical conjugate variables such that $[\hat{\theta}, \hat{n}] = iT$ (we set $\hbar = 1$, thus $T = \hbar_{eff}$). Correspondingly, the quantum dynamics is described by the Floquet operator

$$U = e^{ik(\hat{\theta} - \pi)^2} e^{-iT\hat{n}^2/2}, \quad (2)$$

where $0 < \theta < 2\pi$ and $-N/2 < n \leq N/2$. The wave function time evolution is computed by repeated applications of operator (2) to the initial wave function, *i.e.* $|\psi(m)\rangle = U^m|\psi(0)\rangle$. The dynamics of the QSM is governed by two parameters k, T , while the dynamics of the

*Electronic address: monta@sns.it
URL: www.sns.it/~montangero

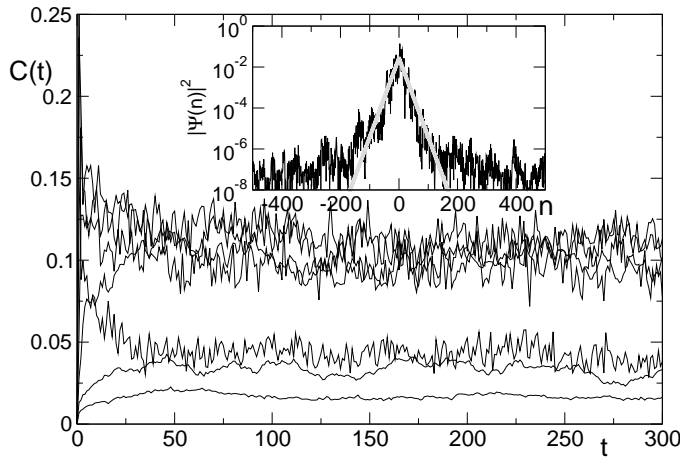


FIG. 1: Concurrence of qubits 1 and 3 as a function of time for different map parameters $K = \sqrt{2}$, $k = K/T$, $T = 2\pi M/2^{n_q}$, $n_q = 10$. From bottom to top $M = 10^4, 5 \cdot 10^3, 3 \cdot 10^2, 2 \cdot 10^3, 5 \cdot 10^2, 10^3, 7 \cdot 10^2$ and $\ell = 0.03, 0.1, 31, 0.7, 11, 2.8, 5.7$ respectively. Inset: peak of an exponentially localized wave function. The grey thick line follows the law (3).

classical correspondent map depends only on the classical parameter $K = kT$ and displays chaotic dynamics for $K > 0$ and $K < -4$ [8]. For $-4 < K < 0$ the map is described by mixed phase space (both integrable and chaotic). The classical limit of map (2) is recovered for $k \rightarrow \infty$ and $T \rightarrow 0$ keeping K constant. For $T \lesssim 1$ and $K > 1$ unique quantum feature appear and QSM displays dynamical localization. The classical chaotic diffusion in momentum is suppressed by quantum interference and the wave function is described by an exponentially localized wavefunction of the form

$$|\psi(n)| \approx e^{-|n|/\ell} / \sqrt{\ell}. \quad (3)$$

The inset of Fig.1 shows such typical localized wave function. Any further evolution of the wave function is suppressed excepted from quantum fluctuations. The QSM in the localized regime is described by the time independent wave function (3) with $\ell \approx \pi^2 k^2 / 3$. Dynamical localization occurs after time $t^* \sim \ell$ [9]. We stress the fact that the expression (3) is a typical signature of quantum chaos. Notice that dynamical localization can be seen only if $\ell \ll N$: In the thermodynamic limit dynamical localization always occurs.

In [13] an efficient quantum algorithm has been presented to simulate the map (2). The algorithm is based on the quantum Fourier transform and it exploits the exponential efficiency of the quantum Fourier transform with respect to the classical fast Fourier algorithm [14]. If performed on a n_q -qubits quantum computer, it needs $O(n_q^2)$ elementary quantum gates, while a classical computer needs $O(N = 2^{n_q})$ elementary gates. Moreover, the QSM algorithm has no need of ancillary qubits: it is already possible to see dynamical localization with less than ten qubits. Notice that any quantum algorithm to simulate a quantum system is based on the introduc-

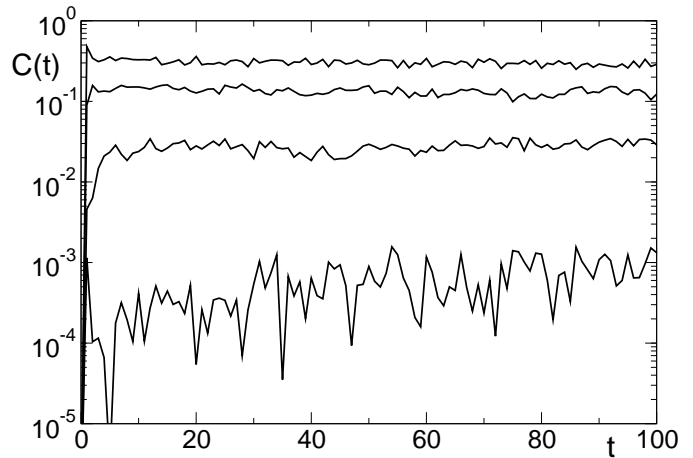


FIG. 2: Concurrence of qubits 1 and j as a function of time for different map parameters $K = \sqrt{2}$, $k = K/T$, $T = 2\pi M/2^{n_q}$, $n_q = 10$, $M = 800$, $\ell = 4.36$. From top to bottom $j = 2, 3, 4, 5$.

tion of the coding of the dynamical variable in binary representation. In our case, the coding is defined by $n = \sum_i \alpha_i 2^i$, where n are the eigenvalues of \hat{n} describing the QSM and $\alpha_i = 0, 1$ depending on which level of the i -th qubit is populated. Thus, the qubits are ordered as they represent different logical values, from the least significant qubit ($i = 1$) to the most significant one ($i = n_q$). Each of them naturally introduce a coarse graining of the space of the n [15]. From now on, we refer to the difference of coarse graining level $\Delta(i, j) = 2^i - 2^j$ as coarse graining distance between the qubits. Moreover, for the sake of simplicity, we will identify the logic label i with the spatial position. However, our results are general as they can be recovered with an appropriate mapping between spatial and logic position. It is common wisdom that entanglement is a necessary resource to exploit the quantum computational gain. It is then natural to study the pairwise entanglement in the qubits that describe a dynamically localized system. We show that pairwise entanglement is present between the qubits and that its value depends by the natural ordering introduced by the quantum algorithm. Indeed, differently from other studies, the coding $n = \sum_i \alpha_i 2^i$, introduce a hierarchy that was not present in spin systems as in [1]. We show that in the regime of dynamical localization the concurrence value exponentially depends on the coding position of the pair of qubits and that it is exponentially sensitive of small change of the kick strength k .

We quantify the pairwise entanglement present between any pair i, j (with $i < j$) of qubits by means of concurrence [16], defined as $C = \max\{\lambda_1 - \lambda_2 - \lambda_3 - \lambda_4, 0\}$, where the λ_i 's are the square roots of the eigenvalues of the matrix $R = \rho^{i,j} \tilde{\rho}^{i,j}$, in descending order; the spin-flipped density matrix is defined by $\tilde{\rho}^{i,j} = (\sigma_i^y \otimes \sigma_j^y)(\rho^{i,j})^*(\sigma_i^y \otimes \sigma_j^y)$ (in this definition the two qubits basis $|\alpha_i \alpha_j\rangle$ must be used). The reduced density matrix

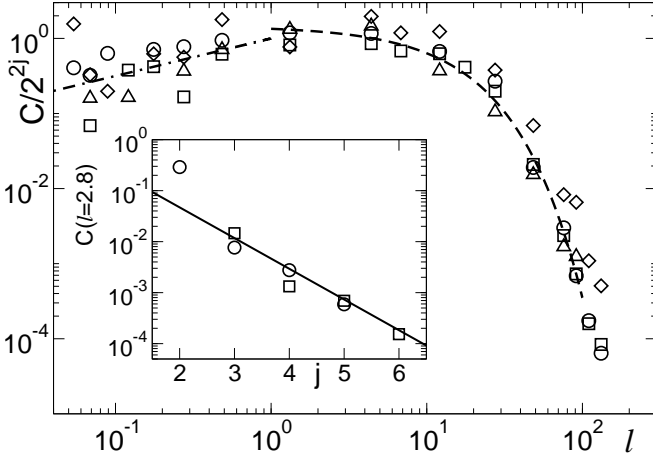


FIG. 3: Concurrence saturation values between qubits $i = 1$ and j as a function of localization length ℓ . Different symbols represents different qubits couples: $j = 2$ (circles), $j = 3$ (squares), $j = 4$ (diamonds), $j = 5$ (triangles). Dashed lines follows the predicted behavior $C(\ell) \sim \ell^{0.5}$ and $C(\ell) \sim \exp(-A\ell)$. Inset: Concurrence values for $\ell = 2.8$ and different qubits couples: $i = 1$ (circles) and $j - i = 1$ (squares). Full line represents $C(j) \sim 2^{-2j}$.

$\rho^{i,j}$ is given by

$$\rho_{l,m}^{i,j}(t) = \prod_{k=1, k \neq i,j}^{n_q} \sum_{\alpha_k=0}^1 A_{\alpha_1 \dots \beta_l \dots \beta_m \dots \alpha_{n_q}}^* A_{\alpha_1 \dots \beta_l \dots \beta_m \dots \alpha_{n_q}} |\psi(t)\rangle \quad (4)$$

where $l, m = 0, 1 \dots 3$, the β_k are the binary code of l and m and $A_{\alpha_1 \dots \beta_l \dots \beta_m \dots \alpha_{n_q}} = \langle \alpha_1 \dots \beta_l \dots \beta_m \dots \alpha_{n_q} | \psi(t) \rangle$.

We start with an initial wave function equal to a momentum eigenstate $|\psi(t=0)\rangle = |n\rangle$, we compute the time evolution at a given time t by repeated application of the Floquet operator (2) and at each time we compute the concurrence by means of the reduced density matrix (4). We plot in Fig.1 the concurrence evolution of two qubits as a function of time for different k values and fixed K : this choice of the parameter values corresponds to the same classical dynamics but different quantum dynamics with different localization time and length. The stationary regime is reached for larger times as ℓ value is increased. In Fig. 2 we plot the concurrence evolution for fixed ℓ and different qubit pairs. The different saturation levels and times are visible. Notice that the concurrence saturation level is not a monotonic function of the localization length: indeed the two limiting situations, a momentum eigenstate and a random superposition of all the momentum eigenstate i.e. an ergodic wave function, have zero concurrence values for any qubit pair [7], thus a maximally entangled case should lie in between.

In Fig. 3 we show in details the saturation value of the concurrence between the less significant bit ($i = 1$) and the others ($j = 2, 3 \dots$) as a function of the localization length. There are two distinct regimes: for $\ell \lesssim 1$ the concurrence increases as $C(\ell) \sim \sqrt{\ell}$, while for $\ell \gg 1$ the concurrence is exponential sensitive to the localization

length. The squared root dependence can be understood as follows: The number of addend different from zero in (4) can be estimated as $N_\ell = \ell/\mathcal{G} = \ell/(\Delta 2^j)$. Indeed, the number of pairs of coefficients $A_{\alpha_1 \dots \beta_l \dots \beta_m \dots \alpha_{n_q}}$ of coarse graining distance $\Delta(i, j)$ in an ensemble of ℓ coefficients different from zero drops linearly with $\Delta(i, j)$, thus exponentially with j . The structure is repeated each 2^j , giving the scaling $\mathcal{G} \sim \Delta 2^j$. For $\ell \lesssim 1$ only few levels of the wave function are significantly populated, and they are “near”, i.e. the binary code of their position n in the wave function $(\beta_1 \alpha_2 \dots \beta_j \dots \alpha_{n_q})$ differs only for the value of β_1 . To estimate the sum (4) we approximate the wave function with the expression

$$|\psi\rangle \approx \sum_{i=\bar{m}}^{\bar{m}+\ell} \frac{e^{i\phi_i}}{\sqrt{\ell}} |i\rangle, \quad (5)$$

where ϕ_i is a random phase and $\bar{m} + \ell/2$ the position of the peak of the wave function [9]. Thus the density matrix will be composed by diagonal terms proportional to $\rho_{k,k}^{i,j} \sim 1/\mathcal{G}$. Notice that either $\rho_{0,0}^{i,j}$ or $\rho_{3,3}^{i,j}$ will be negligible as they have a coarse graining distance is $\Delta \gg \ell$. Equivalently, the off diagonal matrix elements which differ significantly from zero are those who are composed by products of terms which have the smaller coarse graining distance, that is, the first lower and upper diagonal. Furthermore, if $\rho_{3,3}^{i,j}$ is negligible also $\rho_{2,3}^{i,j}$ may be approximate by zero. We then compute the $R_p^{i,j}$ matrix, which mix up the density matrix elements, leading to an approximate two by two matrix of the form:

$$R_p \sim \begin{pmatrix} 0 & 0 & 0 & 0 \\ 0 & \frac{1+\ell}{\mathcal{G}^2} & \frac{\ell}{\mathcal{G}^2} & 0 \\ 0 & \frac{\ell}{\mathcal{G}^2} & \frac{1+\ell}{\mathcal{G}^2} & 0 \\ 0 & 0 & 0 & 0 \end{pmatrix}. \quad (6)$$

The squared root of the non-zero eigenvalue of R_p matrix is then proportional to $\sqrt{\ell}/\mathcal{G} \sim \sqrt{\ell}/2^{2j}$. Equation (6) implies that the saturation value of the concurrence for small ℓ scales as $C \sim \sqrt{\ell}/2^{2j}$: This prediction is in agreement with the numerical data presented in Fig. 3.

For $\ell \gg 1$ the concurrence has a completely different behavior (Fig. 3): the number of coefficients different from zero in (4) increases, the approximation that leads to (6) is not valid any more as the off-diagonal coefficients of (4) start to be not negligible. The overall effect is that the concurrence drops exponentially with ℓ , up to a critical value where it drops exactly to zero. This happens when all the off diagonal term are on average equal. As $\ell \propto k^2$, small changes in the Hamiltonian (1) of the kind $k \rightarrow k + \Delta k$ change exponentially the pairwise entanglement present in the system.

In the inset of Fig. 3 the concurrence saturation values for different qubit pairs are plotted for a given value of the localization length. As it can be clearly seen the points follows the estimate $C(\ell) \propto 2^{-2j}$. In Fig. 4 we show that the two different regimes of the concurrence are typical of any pair of the qubits: For every couple of qubits chosen

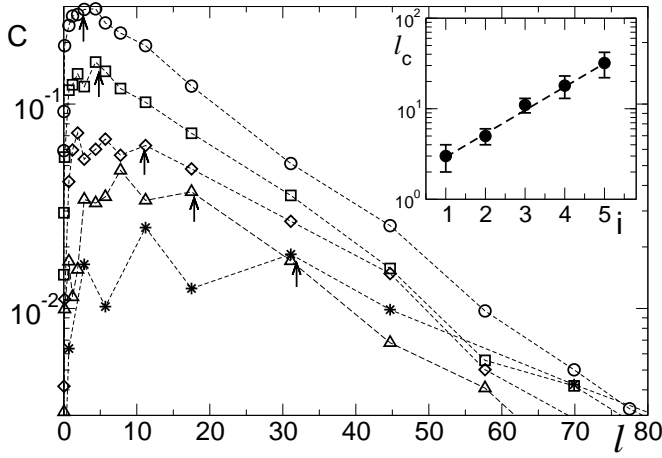


FIG. 4: Concurrence saturation values between qubits i and $j = i + 1$ as a function of localization length ℓ . Different symbols represents different qubits couples: $i = 1$ (circles), $i = 2$ (squares), $i = 3$ (diamonds), $i = 4$ (triangles), $i = 5$ (stars). Arrows point where the exponential decay starts. Inset: ℓ_c as a function of i . The dashed line is an exponential fit.

there is a regime of squared root increasing followed by an exponential decay. Notice that here the critical point ℓ_c where exponential sensitivity starts drastically depend on the couple of qubits chosen. Indeed, $\ell_c \sim 2^i$. This is due to the fact that the number of coefficients in (4) different from zero, scales as $\Delta \sim 2^i$, as the labels of the off-diagonal coefficients that are multiplied differ at least of 2^i . Thus, not negligible off diagonal terms appears for greater values of ℓ . In Fig. 4 this behavior is shown by means of the arrows the predicted points $\ell_c(i) = 2^i$: the value of the localization length corresponding to the maximum concurrence saturation value are shown in the inset of Fig4.

We now focus the bipartite entanglement and we characterize it by means of the Von Neumann entropy of one subsystem. We bipartite the system in two subsystems A and B , each composed by n_A and n_B qubits respectively, we compute

$$S_A = -\text{Tr} \rho_A \log \rho_A, \quad (7)$$

where ρ_A is the reduced density matrix of the subsystem A . Notice that, due to the hierarchy introduced by the binary coding $n = \sum \alpha_i 2^i$, the bipartite entanglement displays very different behaviors depending on which qubits compose the subsystems. It is necessary then to specify both the size and the labels of the qubits in each subsystem. We first bipartite the system in qubits one to m , varying m ($n_A = m$ and $n_B = n_q - m$). Then, we study the case of subsystem A composed of a single qubit ($n_A = 1$ and $n_B = n_q - 1$), varying its position. We evaluate the Von Neumann entropy after the localization time, thus when the wave function of the system can be described by Eq.(3) and S_A is stationary.

In Fig.5 we show the saturation level of the entropy of a

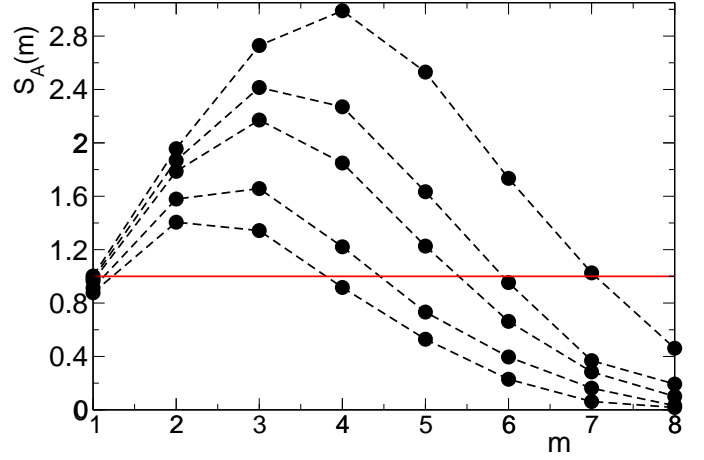


FIG. 5: Von Neumann entropy S_A of a subsystem composed by qubits 1 to m for different value of localization length (from bottom to top $\ell \simeq 2^k$, $k = 4, 5, 6, 7, 8$).

subsystem of size m for different values of the localization length ℓ . We define a critical threshold S_c of the entropy under which we consider the block of m spins unentangled with the others. If we choose $S_c = 1$ (straight line in Fig.5), it is clear that the maximum number of qubits entangled increases as $\log \ell$. It has been shown recently [4] that the feasibility of efficient classical simulations of a quantum system is conditioned by the presence of bipartite entanglement and its scaling behavior with respect to the number of qubits n . Indeed, if the maximum (with respect to the partition) bipartite entanglement in the system scales at maximum as $\log n_q$, it is possible to perform efficient classical simulations. In our system, we may scale the number of qubits keeping fixed the system size, thus exploring smaller and smaller scales of the system ($T \rightarrow 0$), or increasing the system size ($T = \text{const}$). In the former case ℓ grows exponentially with n_q and $S_A \sim n_q$ thus there are no known efficient classical simulation methods, while in the latter case ℓ is constant and it is thus possible to perform efficient classical simulations following [4]. This result should not surprise as increasing the system size while studying a dynamically localized system adds almost no information at all, as the wave function tail are almost not populated (the wave function coefficients decays exponentially). In conclusion, quantum computation of dynamically localized systems do improve the efficiency of classical simulations. However, the improvement to compute interesting quantities as the localization length is only quadratic and not exponential as shown in [3]. The same arguments apply in the simulation of an ergodic quantum chaotic system ($\ell = 2^{n_q}$). Thus, the simulation of a complex many body quantum system, is classically inefficient while it is, at least in principle, possible to simulate it efficiently if an efficient quantum algorithm exists.

In Fig. 6 we perform a different analysis, studying the Von Neumann entropy of a single qubit with respect to the rest of the quantum computer as a function of the

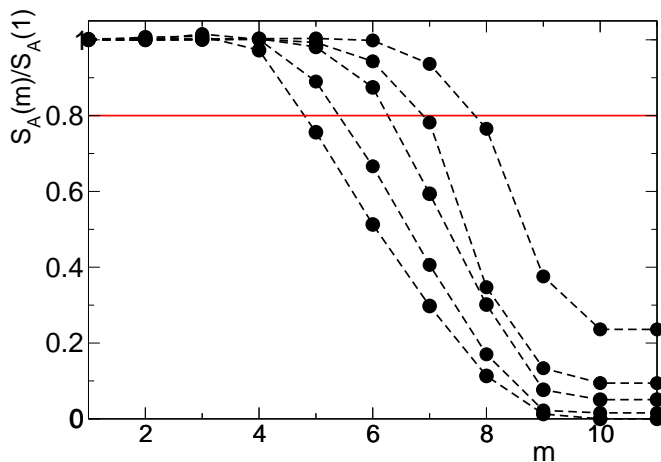


FIG. 6: Von Neumann entropy S_A of a subsystem composed by a single qubit m for different value of localization length (from bottom to top $\ell \simeq 2^k$, $k = 4, 5, 6, 7, 8$).

localization length. The figure shows clearly that the entanglement depends on the position of the qubit. Again, we define a critical threshold under which we consider not entangled the qubit. As before, the number of entangled qubits scales logarithmically with the localization length. Thus, the measure of the reduced density matrix of a single qubit can be used as an efficient method to estimate the localization length of a quantum chaotic system. This estimate is crucial to investigate complex quantum system efficiently by means of both classical and quantum

simulations.

In conclusion we have shown that the concurrence in a quantum computer that simulates a dynamically localized system is exponentially sensitive to both small changes of the Hamiltonian and to the qubits chosen. This sensitivity is due to the natural ordering introduced on the qubit by the coding of the simulated system. Notice that this is a signature of quantum chaos on a pure quantum characteristic with no classical analogue. It should be also interesting to compare such sensitivity with the cases of classical regular and semi-integrable dynamics. Furthermore, the same sensitivity has been found recently in the ground state of a single particle Anderson model [17]: these two results reflects the underlying connections between the dynamical and the Anderson localization, and a better comprehension of this behavior might lay in a more general picture. The results on the Von Neumann entropy showed that, the dynamical regime of the simulated quantum system influence the possibility of performing efficient classical simulations. In the case of a localized state there are no known methods to perform an efficient classical simulation if one is exploring smaller scales while increasing the number of qubits. A more detailed picture of the dependences of the feasibility of efficient quantum simulations depending on the dynamical regime of the system will be the objects of further studies.

The author thanks Rosario Fazio and Giuliano Benenti for interesting discussions and a careful reading of the manuscript.

-
- [1] S. Bettelli, D. L. Shepelyansky Phys. Rev. A **67** 054303 (2003). A. J. Scott, Carlton M. Caves J. Phys. A **36** 9553 (2003). X. Wang, S. Ghose, B. C. Sanders, B. Hu quant-ph/0312047. D. Rossini, G. Benenti, G. Casati quant-ph/0309146.
 - [2] D. Poulin, R. Laflamme, G. J. Milburn, and J. P. Paz Phys. Rev. A **68**, 022302 (2003).
 - [3] G. Casati, S. Montangero “Decoherence and Entropy in Complex Systems”, ed. H.-T. Elze, Lecture Notes in Physics Vol. 633, p. 341, (Springer, Berlin, 2004).
 - [4] G. Vidal Phys. Rev. Lett. **91**, 147902 (2003).
 - [5] F. Haake, “Quantum Signatures of Chaos”, (Springer, 1991).
 - [6] R. A. Jalabert and H. M. Pastawski, Phys. Rev. Lett. **86**, 2490 (2001). P. Jacquod, P. G. Silvestrov and C. W. J. Beenakker, Phys. Rev. E **64**, 055203 (2001). G. Benenti and G. Casati, Phys. Rev. E **66**, 066205 (2002). T. Prosen and M. Znidaric, J. Phys. A **34**, L681 (2001); T. Prosen, T. H. Seligman and M. Znidaric, Prog. Theor. Phys. Supp. **150**, 200 (2003).
 - [7] S. Montangero, G. Benenti, and R. Fazio, Phys. Rev. Lett. **91**, 187901 (2003).
 - [8] O. Chen, I. Dana, J. D. Meiss, N. W. Murray, I. C. Percival, Physica D **46**, 217 (1990). I. Dana, N. W. Murray, I. C. Percival, Phys. Rev. Lett. **62**, 233 (1989).
 - [9] G. Benenti, G. Casati, S. Montangero, D. L. Shepelyansky Phys. Rev. A **67**, 052312 (2003).
 - [10] G. Casati, B. V. Chirikov, J. Ford, F. M. Izrailev, Lecture Notes Phys. **93**, 334 (1979); for a review see, e.g., F. M. Izrailev, Phys. Rep. **129**, 299 (1990).
 - [11] F. L. Moore, J. C. Robinson, C. Bharucha, P. E. Williams, and M. G. Raizen. Phys. Rev. Lett. **73**, 2974 (1994).
 - [12] S. Fishman, D. R. Grempel, and R. E. Prange, Phys. Rev. Lett. **49**, 509 (1982).
 - [13] G. Benenti, G. Casati, S. Montangero, D. L. Shepelyansky, Phys. Rev. Lett. **87**, 227901 (2001).
 - [14] A. Ekert, R. Jozsa, Rev. Mod. Phys. **68**, 733 (1996).
 - [15] M. Terraneo, D. L. Shepelyansky Phys. Rev. Lett. **92**, 037902 (2004).
 - [16] C. H. Bennett, D. P. DiVincenzo, J. A. Smolin, and W. K. Wootters, Phys. Rev. A **54**, 3824 (1996). W. K. Wootters, Phys. Rev. Lett. **80**, 2245 (1998).
 - [17] H. Li, X. Wang, Y. Li quant-ph/0403178.